

# Excess carrier recombination lifetime of bulk *n*-type 3C-SiC

Vytautas Grivickas,<sup>1,a)</sup> Georgios Manolis,<sup>1</sup> Karolis Gulbinas,<sup>1</sup> Kęstutis Jarašiūnas,<sup>1</sup> and Masashi Kato<sup>1,2</sup>

<sup>1</sup>Institute of Applied Research, Vilnius University, Saulėtekio 10, LT-10223 Vilnius, Lithuania

<sup>2</sup>Department of Engineering Physics, Electronics and Mechanics, Nagoya Institute of Technology, Gokiso, Showa, Nagoya 4666-8555, Japan

(Received 10 August 2009; accepted 18 November 2009; published online 16 December 2009)

Transient absorption technique was used to determine carrier lifetimes in 3C-SiC grown on Si and 6H-SiC substrates. A slow lifetime component originated from minority carrier traps and pointed out to the trap saturation with increasing injection. Recombination lifetime in different samples varied between 0.5–120 ns. Its value decreased with excess carrier density in the transition range between minority-carrier-lifetime and high-injection lifetime but abnormally increased above the carrier density of  $2 \times 10^{17} \text{ cm}^{-3}$ . Negligible contribution of surface and Auger recombination to recombination lifetime peculiarities was observed. Possible mechanisms of the observed lifetime variation are discussed. © 2009 American Institute of Physics. [doi:10.1063/1.3273382]

Electrical properties of cubic silicon carbide (3C-SiC) make this polytype an attractive candidate for many high power device applications. Bulk growth of this polytype, however, is complicated as 3C-SiC is the least stable form of SiC with the smallest 2.36 eV indirect band gap among all SiC polytypes. Epitaxial deposition of 3C-SiC layers was suggested on the (001) face of the Si substrates and the (0001) face of the 6H-SiC substrates.<sup>1</sup> During the last decade both growth methods improved substantially and 100  $\mu\text{m}$  thick freestanding *n*-type 3C-SiC wafers with high material purity were demonstrated.<sup>2</sup>

Excess carrier lifetime is a sensitive indicator of a single crystal quality. Exact lifetime values are needed for modeling of electronic devices. In contrast to other polytypes,<sup>3–8</sup> dominant recombination mechanisms in 3C-SiC are poorly understood. Under low-level (LL) excitation ( $\Delta n \ll n_0$ , where  $\Delta n$  and  $n_0$  are the excess and the equilibrium electron concentrations, respectively), carrier decays in 3C-SiC were obtained by microwave<sup>9</sup> and photoconductivity<sup>10</sup> techniques. Both techniques showed that carrier decay is consisting of the initial fast ( $\tau_R \approx 1\text{--}15 \text{ ns}$ ) part and the subsequent slow ( $\tau_S > 1 \text{ ms}$ ) tail. The initial part was assigned to the recombination through active recombination levels while the appearance of the tail was attributed to the minority carrier trapping by the deep band gap centers. The effect of a high build-in strain<sup>11</sup> between the thin 3C-SiC epitaxial layers and the Si substrates was not considered in these studies. Under high-level (HL) excitation ( $\Delta n \gg n_0$ ), excess carrier decays were studied using the four wave mixing (FWM) technique.<sup>12,13</sup> High temporal resolution of these experiments showed the fast decays with the 1–4 ns and, at high carrier concentrations, an increase of the lifetime was registered as opposed to the conventional lifetime decrease owing to the Auger recombination mechanism. In this letter, we report an investigation of carrier recombination processes in thick, freestanding 3C-SiC samples using the time- and spatially resolved free-carrier-absorption (FCA) techniques. A wide injection range, covering transitioning from LL to HL excitation regimes, was achieved in our experiments and thus

allowed to get insight into recombination mechanisms controlling the bulk lifetime of 3C-SiC.

Three different 3C-SiC samples, two grown on the Si substrates and one grown on the 6H-SiC substrate, were investigated in this work. Free standing wafers were obtained by removing the substrates with chemical etching and/or mechanical polishing. The bulk sample growth is described in Ref. 13. Sample labeling, wafer thicknesses  $d$ , and concentrations  $n_0$  at room temperature are provided in Table I. The inset of Fig. 1 shows schematically the two measurement geometries used in the pump-probe experiments. In the or-

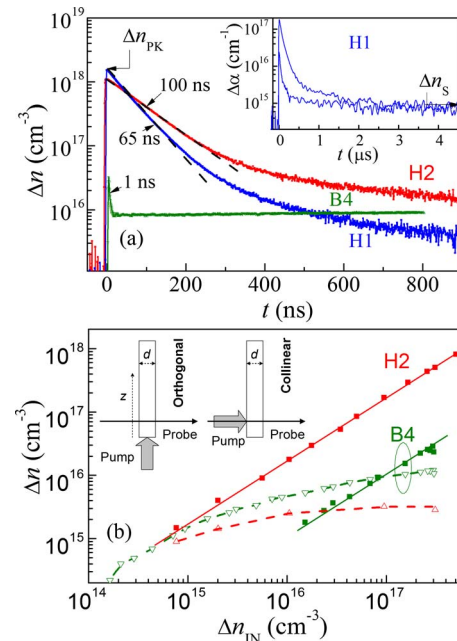


FIG. 1. (Color online) (a) Transient concentration  $\Delta n(t)$  in 3C-SiC samples at injection density of  $10^{18} \text{ cm}^{-3}$ , when excited by 2.384 eV energy photon pulses at 295 K. Exponential fit is applied to the initial decay. In the inset, two transients on H1 sample are shown for lower injections over a longer time scale. (b) Injection dependences of transient concentration magnitude at 77 K excited by 2.53 eV. Peak concentration  $\Delta n_{PK}$  (squares) and saturated concentration  $\Delta n_S$  (triangles) is shown for H2 and B4 samples. Inset shows experimental configuration for measurement under orthogonal and collinear geometries.

<sup>a)</sup>Electronic mail: vytautas.grivickas@ff.vu.lt.

thogonal geometry, used for excitations up to  $2 \times 10^{18} \text{ cm}^{-3}$ , the cross-cut side of 3C-SiC wafer was homogeneously excited with a 2 ns duration laser pulse. Nearly constant distribution of excited carriers was achieved along the  $z$ -direction of the wafer by tuning the excitation wavelength close to the band gap of 3C-SiC. The induced excess carrier dynamics was detected by the FCA decay,  $\Delta\alpha(t, z)$ , of the continuous probe beam propagating perpendicularly to the excited lateral surface. Concentration of the excess electron and hole ( $e$ - $h$ ) pairs was directly proportional to the induced absorption changes:  $\Delta n(t, z) = \Delta\alpha(t, z) / \sigma_{\text{eh}}$ , where the FCA cross-section  $\sigma_{\text{eh}} = 1.4 \times 10^{-17} \text{ cm}^2$  was obtained for the  $1.54 \text{ }\mu\text{m}$  wavelength probe beam using the established calibration procedure.<sup>14</sup> Scans along the  $z$ -direction were obtained while the resolution of the probe beam within the sample was  $8 \text{ }\mu\text{m}$ . In the collinear geometry, used for excitations above  $2 \times 10^{18} \text{ cm}^{-3}$ , both pump and probe beams were directed to the same point on the wafer surface. Excitation was done with a different laser generating 25 ps duration pulses at 351 nm wavelength and probing was done with an optically delayed probe beam at  $1.05 \text{ }\mu\text{m}$  wavelength. The induced absorption changes,  $\Delta\alpha(t)$ , were detected by delaying the probe pulses with respect to the excitation pulses where  $\sigma_{\text{eh}} = 1 \times 10^{-17} \text{ cm}^2$  was set for the  $1.05 \text{ }\mu\text{m}$  wavelength. An integrated injected carrier concentration  $\Delta n_{\text{IN}}$  values of  $e$ - $h$  pairs was calculated using the known photon flux at the sample surface and the known absorption coefficient  $\alpha$  of the excitation wavelength. For 351 nm wavelength the absorption depth  $\alpha^{-1}$  is about equal to about  $5 \text{ }\mu\text{m}$ .<sup>12,13</sup>

Figure 1(a) shows carrier decays detected in all three samples at the injected carrier concentration of  $\Delta n_{\text{IN}} \approx 10^{18} \text{ cm}^{-3}$ . In the H1 and H2 samples, grown on the Si substrates, the initial part of the decays was almost a single exponent with the excess carrier recombination lifetimes  $\tau_R$  in the order of 100 ns. At longer times, the decays diverged into the slow milliseconds component initiating at the saturated  $\Delta n_S$  concentration [see the inset of Fig. 1(a)]. In the B4 sample, grown on the 6H-SiC substrate, the peak measured concentration,  $\Delta n_{\text{PK}}$ , was much smaller than  $\Delta n_{\text{IN}}$  indicating that  $\tau_R$  is comparable to the duration of the excitation laser pulse. The initial fast decay was again followed by the slow milliseconds component with the  $\Delta n_S$  magnitude values substantially higher than in the H1 and H2 samples. Figure 2(b) shows  $\Delta n_{\text{PK}}$  (solid symbols) and  $\Delta n_S$  (open symbols) in the H2 and B4 samples plotted versus  $\Delta n_{\text{IN}}$ . In both samples  $\Delta n_{\text{PK}}$  was linearly dependent on  $\Delta n_{\text{IN}}$ , while  $\Delta n_S$  was saturating at higher  $\Delta n_{\text{IN}}$ . Gradual saturation behavior is typical for minority carrier trapping by deep band gap centers.<sup>6,9,10</sup> The  $\Delta n_S$  limit at high injected concentrations was equated to the total density of filed traps,  $N_T$ , assuming that the electron is dominating the FCA cross-section:  $\sigma_e \approx \sigma_{\text{eh}}$ . The  $N_T$  values are presented in Table I.

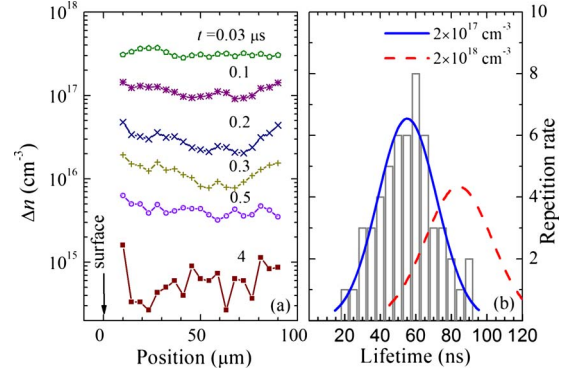


FIG. 2. (Color online) (a) Z-distributions of  $\Delta n(t, z)$  at different times after 2.48 eV photon pulse excitation in H1 sample at 295 K. Z(0) position matches to the excited surface. (b) Histogram of  $\tau_R$  values from different locations and the corresponding Gaussian fit for two indicated injection concentrations  $\Delta n_{\text{IN}}$ .

Effect of surface recombination to the measured  $\tau_R$  values was evaluated using  $z$ -scans of carrier decays.<sup>6,7</sup> Figure 2(a) shows  $\Delta n(t, z)$  profiles detected along the  $z$ -direction of the H1 sample at different moments after the excitation pulse ( $\Delta n_{\text{IN}} \approx 3 \times 10^{17} \text{ cm}^{-3}$ ). No tangible reduction of  $\Delta n$  at  $10 \text{ }\mu\text{m}$  distance from the surface was observed during the decay times equating several  $\tau_R$ . The carrier decay diffusion profile evolution was simulated through the one-dimensional model<sup>15</sup> using the measured ambipolar carrier diffusion coefficient value  $D_a \approx 3.3 \text{ cm}^2/\text{s}$ .<sup>13</sup> The calculations showed that the upper limit of surface recombination rate  $S$  is  $10^3 \text{ cm/s}$ . This value is smaller than the  $10^3$ – $10^5 \text{ cm/s}$  range of rates determined for the mechanically polished surfaces of 4H- and 6H-SiC polytypes<sup>7</sup> and does not significantly affect the measured  $\tau_R$  values in 3C-SiC. Statistical distribution of lifetimes at different sample places was also evaluated using  $z$ -scans. Vertical bars in Fig. 2(b) show  $\tau_R$  distribution in the H1 sample obtained during the  $20 \text{ }\mu\text{m}$  step along the  $z$ -direction. The detected distribution was well fitted using the Gaussian function as shown by the solid line. The same Gaussian distribution was characteristic for higher  $\Delta n_{\text{IN}}$  as illustrated by the dashed line. Statistical lifetime averages and their spreads at the FWHM are provided in Table I for all samples at  $\Delta n_{\text{IN}} = 2 \times 10^{17} \text{ cm}^{-3}$ . The detected ratio between the average values and their spreads compares to the results obtained in the other polytypes of SiC.<sup>7</sup>

Dominant recombination mechanisms in 3C-SiC were determined from the  $\tau_R$  measurements at different  $\Delta n_{\text{IN}}$ . In order to separate these changes from the statistical  $\tau_R$  variations within the sample, special care was taken probing samples at the same position. Figure 3 shows  $\tau_R(\Delta n_{\text{IN}})$  dependence measured in H1 (triangles) and H2 (squares) samples at 295 K (open symbols) and 77 K (solid symbols). The circled symbols in the figure show the precise  $\tau_R$  value

TABLE I. Sample labeling and basic parameters at room temperature.

Sample	Thickness $d(\mu\text{m})$	Equilibrium density $n_0(\text{cm}^{-3})$	$\tau_R(\text{ns})$ at $\Delta n = 2 \times 10^{17} \text{ cm}^{-3}$	Trap density $N_T(\text{cm}^{-3})$
H1 (on Si)	255	$(3-5) \times 10^{15}$	55 (spread $\pm 17$ )	$(7-10) \times 10^{14}$
H2 (on Si)	160	$(1-3.5) \times 10^{17}$	88 (spread $\pm 42$ )	$3.6 \times 10^{15}$
B4 (on 6H-SiC)	800	$N = (1-5) \times 10^{16} \text{ at/cm}^3$	0.8	$1.45 \times 10^{16}$

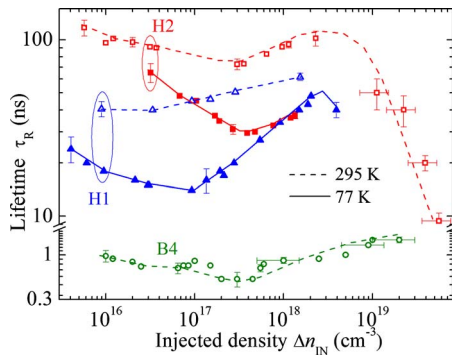


FIG. 3. (Color online) Recombination lifetime  $\tau_R$  vs excess carrier density in three 3C-SiC samples. Dashed and solid line is the guide for the eye for injection dependences at 295 K and at 77 K, respectively.

of the initial fast decay of the B4 sample at room temperature, which were determined by the FWM technique.<sup>13</sup> The steep decrease of lifetime observed in the H2 sample at 295 K above  $10^{19} \text{ cm}^{-3}$  appeared due to the Auger recombination. The  $\gamma = 2.5 \times 10^{-32} \text{ cm}^6/\text{s}$  Auger coefficient was extracted from the  $\gamma = (\tau_R \times \Delta n^2)^{-1}$  data fits.<sup>16</sup> This  $\gamma$  value was found thirty times smaller than the one obtained in the 4H-SiC polytype.<sup>7</sup> The result can be explained by the difference in the band structures of the two polytypes. In the direct  $e$ - $e$ - $h$  Auger process, the  $2E_g(X_{1C}-\Gamma_{15V}) \geq E_g(\Gamma_{1C}-\Gamma_{15V})$  requirement has to be satisfied, where  $E_g(X_{1C}-\Gamma_{15V})$  is the indirect band gap and  $E_g(\Gamma_{1C}-\Gamma_{15V})$  is the direct gap at the  $\Gamma$ -symmetry point. While this requirement is almost fulfilled in 4H-SiC polytype, there is  $\sim 1.3 \text{ eV}$  deficit in the band structure of the 3C-SiC polytype. Therefore, the weak phonon-assisted Auger process is the most likely recombination mechanism in 3C-SiC at high injections.

In the  $\Delta n_{IN}$  range  $5 \times 10^{15} - 5 \times 10^{18} \text{ cm}^{-3}$ , the  $\tau_R$  dependency in all samples at room temperature had a V-shape. This dependency became even more pronounced in H1 and H2 samples at 77 K. The standard Shockley-Read-Hall (SRH) theory for a single recombination center in a forbidden gap can explain only S-shape (deep center) or a reverse S-shape (shallow center) dependencies.<sup>17</sup> The same theory for two noninteracting deep and shallow centers can explain mixed injection dependency which produces namely the  $\Lambda$ -shape. Such lifetime nonlinearity was demonstrated in p-type Si, where simultaneous recombination through the Fe interstitial impurity and the FeB acceptor-pair was observed.<sup>18,19</sup> In addition, according to the SRH theory a lifetime peak should occur around the LL/HL transition ( $\Delta n \sim n_0$ ) on  $\Lambda$ -shape injection dependencies. This contradicts the clear shift of the lifetime minima on V-shape in 3C-SiC to the higher  $\Delta n_{IN}$  values with decreasing temperature (Fig. 3), while the substantial  $n_0$  reduction by factor of 1/20 is measured with decreasing temperature to 77 K in moderately doped  $n$ -type 3C-SiC.<sup>2</sup>

It is believed that recombination in 3C-SiC should occur through the defect level similar to the  $Z_1/Z_2$  center detected in 4H-SiC.<sup>3,5,8</sup> This center originates from the carbon

vacancy-related complexes on the cubic and hexagonal sites and dominates an intrinsic lifetime of the 4H-SiC polytype. Despite the complicated injection dependent nature of the center, which has three possible charge states, the constant HL-lifetime values are observed in 4H-SiC before up to the onset of the Auger recombination.<sup>7,8</sup> We speculate that the V-shape dependency in 3C-SiC originates from the dynamic capture barrier for the majority electrons due to the lattice relaxation around the different charge states of this defect. In 4H-SiC polytype deep level transient spectroscopy measurements showed that the  $Z_1/Z_2$  center has the large minority hole capture cross-section  $s_h \approx 10^{-14} \text{ cm}^2$  and two electron capture cross-sections of the order  $s_e \geq 10^{-15} \text{ cm}^2$ . Using these values and the simple  $\tau_{HL} \approx (v_{th} \times s_e \times N_R)^{-1}$  relation, where  $v_{th}$  is the thermal velocity and  $N_R$  is the defect concentration, we estimate that  $N_R \approx 10^{14} - 10^{15} \text{ cm}^{-3}$  in the H1 and H2 samples, and  $N_R \approx 10^{16} \text{ cm}^{-3}$  in the B4 sample. These values are by one or two orders of magnitude higher than the ones observed in high quality 4H-SiC epilayers.

This work is supported by the EU FP6 Contract No. MRTN-CT-2006-35735, by the Swedish Visby program, and by Lithuanian State and Studies Foundation. We also thank Professor J. Linnros for access to experimental equipment at Royal Institute of Technology.

- <sup>1</sup>R. F. Davis and J. T. Glass, *Advances in Solid State Chemistry* (JAI, Oxford, 1991), Vol. 2, pp. 1–111.
- <sup>2</sup>T. Yamada and K. M. Itoh, *Mater. Sci. Forum* **389–393**, 675 (2002).
- <sup>3</sup>M. Kawai, T. Mori, M. Kato, M. Ichimura, S. Sumie, and H. Hashizume, *Mater. Sci. Forum* **556–557**, 359 (2007).
- <sup>4</sup>S. A. Reshanov, K. Schneider, R. Helbig, G. Pensl, H. Nagasawa, and A. Schöner, *Mater. Sci. Forum* **457–460**, 513 (2004).
- <sup>5</sup>J. P. Bergman, *Diamond Relat. Mater.* **6**, 1324 (1997).
- <sup>6</sup>P. Grivickas, A. Galeckas, J. Linnros, M. Syväjärvi, R. Yakimova, V. Grivickas, and J. A. Tellefsen, *Mater. Sci. Semicond. Process.* **4**, 191 (2001).
- <sup>7</sup>A. Galeckas, J. Linnros, M. Frichholz, and V. Grivickas, *Appl. Phys. Lett.* **79**, 365 (2001).
- <sup>8</sup>P. B. Klein, *J. Appl. Phys.* **103**, 033702 (2008).
- <sup>9</sup>M. Ichimura, H. Tajiri, Y. Morita, N. Yamada, and A. Usami, *Appl. Phys. Lett.* **70**, 1745 (1997).
- <sup>10</sup>M. Ichimura, N. Yamada, H. Tajiri, and E. Arai, *J. Appl. Phys.* **84**, 2727 (1998).
- <sup>11</sup>A. Galeckas, A. Yu. Kuznetsov, T. Chassagne, G. Ferro, J. Linnros, and V. Grivickas, *Mater. Sci. Forum* **457–460**, 657 (2004).
- <sup>12</sup>K. Neimontas, K. Jarašiūnas, M. Soueidan, G. Ferro, and Y. Monteil, *Mater. Sci. Forum* **556–557**, 395 (2007).
- <sup>13</sup>G. Manolis, K. Jarašiūnas, I. G. Galben, and D. Chaussende, *Mater. Sci. Forum* **615–617**, 303 (2009).
- <sup>14</sup>P. Grivickas, V. Grivickas, and J. Linnros, *Phys. Rev. Lett.* **91**, 246401 (2003).
- <sup>15</sup>V. Grivickas, L. Linnros, A. Vigelis, J. Šečkus, and J. A. Tellefsen, *Solid-State Electron.* **35**, 299 (1992).
- <sup>16</sup>K. Jarašiūnas, P. Ščajev, V. Gudelis, P. B. Klein, and M. Kato, *Int. Conf. on SiC and Related Materials*, Technical Digest, Paper I-148, Nurnberg, 2009.
- <sup>17</sup>J. Linnros, *J. Appl. Phys.* **84**, 275 (1998).
- <sup>18</sup>D. Macdonald, A. Cuevas, and J. Wong-Leung, *J. Appl. Phys.* **89**, 7932 (2001).
- <sup>19</sup>D. Macdonald and A. Cuevas, *Phys. Rev. B* **67**, 075203 (2003).